Available online at www.sciencedirect.com
SCIENCE DIRECT
Polymer 46 (2005) 6308–6315
polymer
www.elsevier.com/locate/polymer

Singlewall carbon nanotubes covered with polypyrrole nanoparticles by the miniemulsion polymerization

Hyeong Taek Ham[a], Yeong Suk Choi[b], Namjo Jeong[c], In Jae Chung[a,*]

[a]*Department of Chemical and Biomolecular Engineering, KAIST, 373-1, Guseong-dong, Yuseong-gu, Daejeon 305-701, South Korea*
[b]*Fuel-cell Program Team, SAIT (Samsung Advanced Institute of Technology), Mt. 14-1, Nongseo-Ri, Giheung-Eup, Yongin-Si, Gyeonggi-do, South Korea*
[c]*Korea Institute of Energy Research (KIER), 71–2, Jang-dong, Yuseong-gu, Daejeon, 305–343, South Korea*

Received 11 April 2005; received in revised form 16 May 2005; accepted 18 May 2005
Available online 24 June 2005

Absract

Singlewall carbon nanotubes were covered with polypyrrole via in situ miniemulsion polymerization of pyrrole monomer. They had nanotube surfaces partially enveloped with polypyrrole: the surfaces attached with polypyrrole particles, the surfaces covered with thin polypyrrole film, and bare surfaces. The nanotubes covered with polypyrrole were doped with $LiClO_4$ and mixed with a binder, Kynar FLEX 2801, to make composite electrode for supercapacitor. The pelletized powder of the composite with Li^+ ions exhibited higher electrical conductivity and lower percolation threshold concentration than pristine polypyrrole. The composite was used to fabricate the electrode in supercapacitor without adding other conducting material like carbon black. It showed higher specific capacitance than polypyrrole/binder/carbon black composite. This could be explained due to the existence of bare surfaces of SWNTs with high electrical conductivity as well as large surface area.

Keywords: Polypyrrole; Singlewall carbon nanotubes; Miniemulsion polymerization

1. Introduction

Singlewall carbon nanotubes (SWNTs) are of great interest for many potential applications in nanoscale devices and materials, field emissions, nanowires, nanotransisters, actuators, hydrogen storage, scanning probe microscopes, and conductive high strength composite materials, since the discovery of SWNTs by Iijima in 1993 [1–8]. Despite of their remarkable properties, the fundamental problems of SWNTs, such as requirement of binder or supporting materials for making film, insolubility in any solvents, and incompatibility with other molecules, act as an obstacle to the progress with SWNTs. So, many efforts have been focused on the functionalization and decoration of SWNT sidewall with other molecules to enhance the solubility in various solvents and the compatibility of SWNTs with other materials [9–11]. Opening up the carbon nanotube ends and encapsulating with other molecules to form a nanocomposite might be used for stable dispersion, separation, and storage technology and for the development of magnetic and electrical properties [12–14].

Electronically conducting polymers (ECPs) have attracted much attention for their low cost and high specific capacitance as electrode materials in supercapacitors [15–19]. Supercapacitors are characterized by high capacitances, which can be implicated in high current load devices. Energy storage in supercapacitors with ECPs is not electrostatic in origin as in double layer capacitor, but is due to a Faradaic process which involves the entire polymer mass [18,19]. Doping–undoping process of ECPs involves the charge–discharge capacitance of the supercapacitor. Supercapacitors based on p- and n-dopable conducting polymers (polyaniline, polythiophene, and polypyrrole) are very attractive for the electric devices with high energy and high power like electric vehicle applications [18–20]. The electrodes are usually composed of composite materials with binders, ECPs, and conductive carbon materials. The conductive carbon materials are used to compensate the relatively low electrical conductivity of ECPs. But they show the low specific capacitance of the supercapacitors.

* Corresponding author. Tel.: +82 42 869 3916; fax: +82 42 869 3910.
E-mail address: chung@kaist.ac.kr (I.J. Chung).

0032-3861/$ - see front matter © 2005 Elsevier Ltd. All rights reserved.
doi:10.1016/j.polymer.2005.05.062

Table 1
The composition of materials for the polymerization and sample codes of PPySWNTs

Sample code	Charged monomer weight		Total monomer weight (g)	Nanotube weight (g)	Weight ratio of nanotube to total monomer (%)	Initiator APS (g)
	Pyrrole (g)	DVB (g)				
PPy	3.0	0	3.0	0.0	0.0	0.340
PPyDVB	2.7	0.3	3.0	0.0	0.0	0.306
Py9D1	0.9	0.1	1.0	0.2	20	0.102
Py18D2	1.8	0.2	2.0	0.2	10	0.204
Py20D0	2.0	0.0	2.0	0.2	10	0.227
Py27D3	2.7	0.3	3.0	0.2	6.7	0.306
Py36D4	3.6	0.4	4.0	0.2	5	0.408

The letters Py and D denote pyrrole and DVB, respectively. The number followed by Py and D stand for the decigram of each material.

Carbon nanotubes are also attractive for the electrode of electrochemical energy storage devices with the use of electrochemical double-layer charge injection [21,22]. Their low mass density, low resistivity, high chemical stability, and large surface area give a big potential for electrodes [22–25]. Especially their large surface area and high aspect ratio make them to have many accessible mesopores. Some experiments have advanced to use carbon nanotubes as a template of ECPs with porous structure to make the surface area of ECPs larger [25–27]. Encapsulation of carbon nanotubes with ECPs was used to get the high electrical conductivity of the electrode as well as the high charge capacity of supercapacitor.

We chose a miniemulsion polymerization among various emulsion polymerization methods, because the method could help us to produce nano-scale polymer particles [28,29]. The method involved a free-radical polymerization in monomer-swollen micelles with an average diameter from one to several hundred nanometers stabilized by surfactants and hydrophobes in oil-in-water system [30,31]. Hydrophobes was used to prevent the Oswald ripening, that is, the growth of miscelles in size and to have many small pores in polymer particles. This miniemulsion polymerization has become useful methods to prepare polymer nanoparticle and polymeric encapsulation of nanoparticles [32,33].

We present the preparation of polypyrrole/SWNT composites (PPySWNTs) by miniemulsion polymerization of pyrrole and their usage as an electrode in supercapacitor. They will have the higher electrical conductivity than ECPs, if there may exist the bare surface of SWNTs because SWNTs have the higher electrical conductivity than ECPs. The experiment was carried out by using various weight ratio of polypyrrole to SWNT content. The electrical and electrochemical property of composites were measured and compared to those of polypyrrole.

2. Experimental

2.1. Materials

AP grade singlewall carbon nanotubes (SWNTs) were purchased from Carbon Nanotechnologies Inc. Dodecyl sulfate, sodium salt (SDS), 1-pentanol, acetone, hydrochloric acid, and divinylbenzene (DVB) were purchased from Aldrich and were used as received. Ammonium persulfate (APS), a free-radical initiator, and pyrrole monomer were purchased from Aldrich Co. and used without further purification. The lithium perchlorate ($LiClO_4$) as lithium salt, and ethylene carbonate (EC) and dimethyl carbonate (DMC) as solvents, were purchased from Aldrich Co. and used as received. The Elf Atochem Co. supplied the Kynar FLEX 2801, poly(vinylidene fluoride-*co*-hexafluoropropylene) P(VdF-*co*-HFP), and the MMM Carbon Co. supplied Super P black, carbon black, for this experiment. The P(VdF-*co*-HFP) and carbon black were dried for 3 days at 40 °C under vacuum before use.

2.2. Polymerization

Before polymerization, the SWNTs were purified by a method described below. SWNTs were thermally treated to remove amorphous carbons at 300 °C for 1 h in the air atmosphere, and then they were stirred in concentrated hydrochloric acid for 10 h to remove the metal catalysts contained in them. The color of the liquid phase turned into green, as the metal catalyst was oxidized. The green color liquid was separated by using the filtration through 200 nm pore membrane. It was treated thermally and chemically with hydrochloric acid for several times until its color became colorless. Finally, SWNTs were dispersed in water to remove water-soluble impurities.

Purified 0.2 g of SWNTs was dispersed with SDS and 1-pentanol in 300 ml of deionized water and then sonicated for 10 h. SDS and 1-pentanol were used as a surfactant and a hydrophobe, respectively. Pyrrole and DVB used as a monomer and a cross-linking agent were mixed before polymerization. This mixture was charged with SWNT aqueous dispersion into a 500 ml three-neck glass reactor equipped with a condenser, a dropping funnel, a stirrer, and a nitrogen inlet. The mixture was then sonicated in nitrogen atmosphere at 0 °C for 4 h, to disperse the nanotubes with monomer. It was kept for 4 h after the 1 M initiator water was dropped through a funnel for 1 h to initiate the

Table 2
Polymer and SWNTs contents in each sample calculated from the residue of TGA curves at 800 °C under N_2 atmosphere

Sample	Polymer contents (wt%)	Nanotube contents (wt%)	Initial weight ratio of nanotubes to total weight (%)
Py9D1	70.75	29.25	16.67
Py18D2	84.76	15.24	9.09
Py20D0	88.48	11.52	9.09
Py27D3	91.30	8.70	6.25
Py36D4	92.43	7.57	4.76

polymerization. The concentration of reactants was listed in Table 1. And then, methanol was added into the flask to terminate the polymerization. The product was mixed with methanol and centrifuged at 8000 rpm for 1 h to remove the surfactants and residual monomer. It was repeated more than five times. The sample was dried under a high vacuum at 60 °C for 3 days. The amount of polypyrrole was determined by using thermogravimetric analyses (Table 2).

2.3. Electrical and electrochemical properties

For the ionic doping of all the samples with lithium perchlorate ($LiClO_4$), EC and DMC were used as solvents and $LiClO_4$ as lithium salt. The powder sample was immersed in 1 M $LiClO_4$ in EC/DMC (1:1 mol/mol) solution, and then stirred for 72 h at room temperature. The doped sample was filtered with 450 nm pore membrane and dried for 48 h at 80 °C under vacuum. To determine the dc conductivity, a four-probe method was used. The pellet of polypyrrole covering SWNTs (PPySWNTs) was made by pressing the powders and its conductivity was measured. The electrical conductivity was also checked for the thin film made by casting the slurry of PPySWNTs and Kynar FLEX 3801 (binder) in acetone. Cyclic voltammograms were evaluated for the slurry cast on platinum disk (area = 0.25 cm^2).

2.4. Measurements

Fourier transform infrared spectra (FTIR) were recorded on a Bomem 102 FTIR spectrometer with KBr pellets. A total of 20 scans taken at 4 cm^{-1} of resolution were averaged.

^{13}C cross-polarized magic angle spinning (CP/MAS) NMR spectra were collected using a Bruker DSX 400 MHz NMR spectrometer in solid state at the Korea Basic Science Institute located in Daegu city. The NMR signal was received with a spin rate of 6 or 8.5 kHz to determine the spinning side bands. The cross-polarized time was 2–3 ms and the delay time was 3 s.

Thermogravimetric analyses (TGA) were carried out with a Perkin–Elmer thermobalance from room temperature to 800 °C, with a rate of 10 °C/min under N_2 and air atmosphere.

The morphology of the nanotubes was examined by a Philips XL30SFEG scanning electron microscope (SEM) with Schottky based field emission gun and by a Philips CM-20 transmission electron microscope (TEM). Surface distribution of polypyrrole was determined by a Philips 535M with energy dispersive spectroscopy (EDS).

The electrical and electrochemical properties of PPySWNTs were measured. Electrical conductivity was examined four point probe head CMT-SR1000 of Changmin Co. Cyclic voltammetry (CV) has been used to characterize

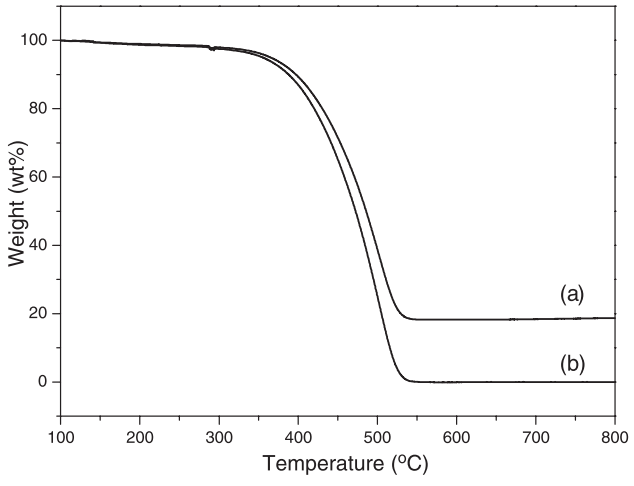

Fig. 1. Thermal gravimetric curves for (a) raw SWNTs and (b) Purified SWNTs.

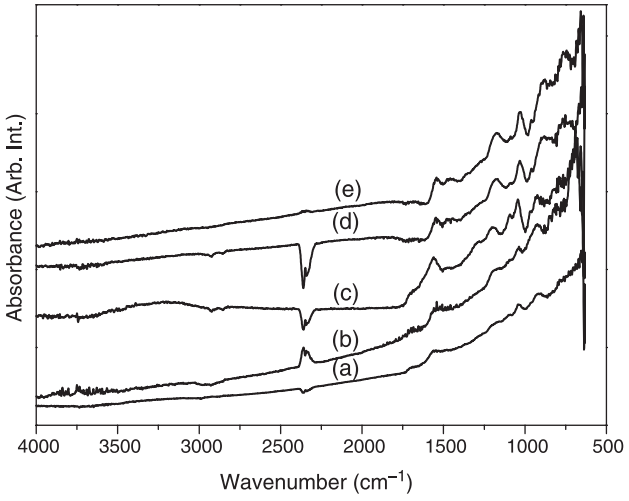

Fig. 2. FTIR spectra of (a) Py09D1, (b) Py18D2, (c) Py20D0, (d) Py27D3, (e) Py36D4.

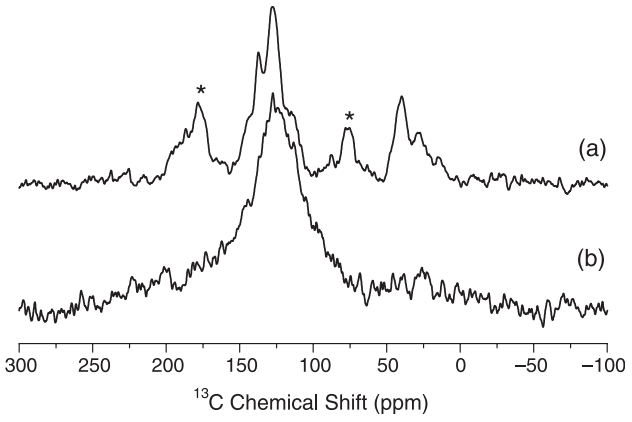

Fig. 3. ^{13}C CP/MAS NMR spectrum of (a) PPyDVB and (b) PPy. Spinning speed was 8.5 kHz. Spinning side bands are indicated by *.

the redox behavior and the kinetic reversibility of the cell. Cyclic voltammograms were recorded by employing a Hokuto Denko HA-301 potentiostat/galcanostat with *X–Y* recorder. A platinum plate with PPySWNTs was used as a working electrode. The counter and reference electrodes were platinum and silver, respectively.

3. Results and discussion

The supplied SWNTs were purified by thermal and concentrated HCl treatment before polymerization. The weight fraction of impurities in SWNTs samples was determined by thermogravimetric analysis (TGA) under air atmosphere. Fig. 1 shows thermal degradation of carbon nanotubes. SWNTs degraded around 350–600 °C under air atmosphere. The amount of metal catalysts removed during purification with HCl was determined using the residual weight difference between the raw SWNTs and the purified SWNTs at 600 °C. The residual weight percentage of catalysts was 18 wt% for raw SWNTs, and almost 0 wt% for purified SWNTs. This reveals that most catalysts in the sample were removed during purification [34].

The synthesized polymer was characterized with FTIR and NMR spectrum. Fig. 2 shows the FTIR spectra of PPySWNTs. The peaks around 1550 and 1450 cm^{-1} were due to aromatic C=C and C–C in polypyrrole, respectively. C=N, and C–N show peaks around 1182 and 1300 cm^{-1}. Aromatic C–H in polypyrrole shows the peak at 1036 cm^{-1}. These peaks illustrate that polypyrrole was polymerized. The peaks from DVB do not show clearly and partially overlapped.

^{13}C CP/MAS NMR spectra were also collected to evaluate the synthesis of the copolymer of pyrrole and DVB (PPyDVB) [35,36]. Polypyrrole (PPy) shows only one broad peak at 100–150 ppm in Fig. 3. It is caused by the overlap of the peaks assigned to quaternary aromatic carbons (=C<) and protonated chromatic carbons (=CH–) in Fig. 3(b). PPyDVB, synthesized copolymer of pyrrole and divinylbenzene, also shows the same broad overlapped peak at 100–150 ppm. And there is another peak around 40–50 ppm caused by the configurational and conformational heterogeneity of aliphatic methylene carbons.

The inset graph in Fig. 4 is the thermogravimetric curves of purified SWNTs, PPy and PPyDVB under N_2 atmosphere. SWNTs do not degrade until the temperature reaches 800 °C under N_2 atmosphere. The main chain of polypyrrole (PPy) decomposes at around 500 °C and almost all the polymers decompose at 800 °C, as shown in Fig. 4. PPyDVB shows multiple peaks at 230 and 450 °C. The

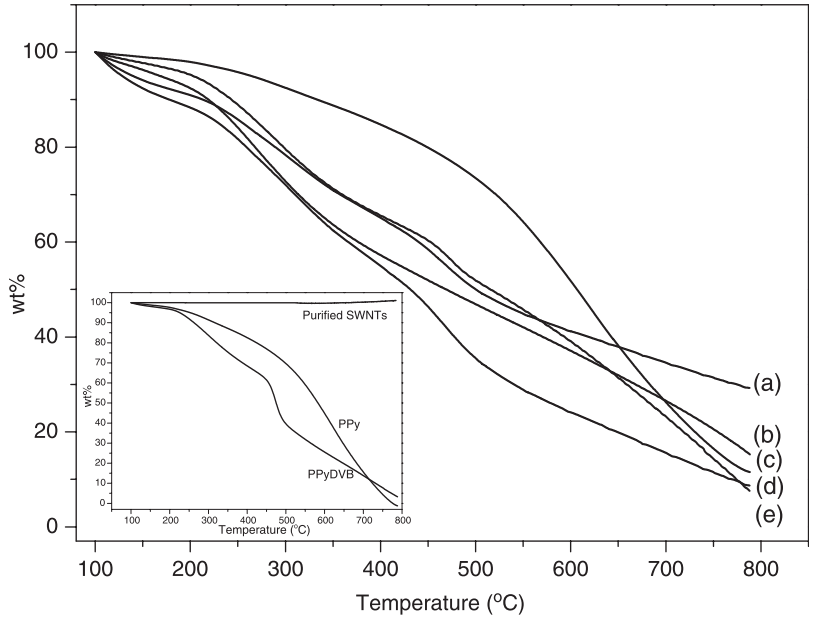

Fig. 4. Thermal gravimetric curves for (a) Py9D1, (b) Py18D2, (c) Py20D0, (d) Py27D3, (e) Py36D4. Inset figure represents TGA curves for purified SWNTs, copolymer of polypyrrole and divnylbenzene, and polypyrrole.

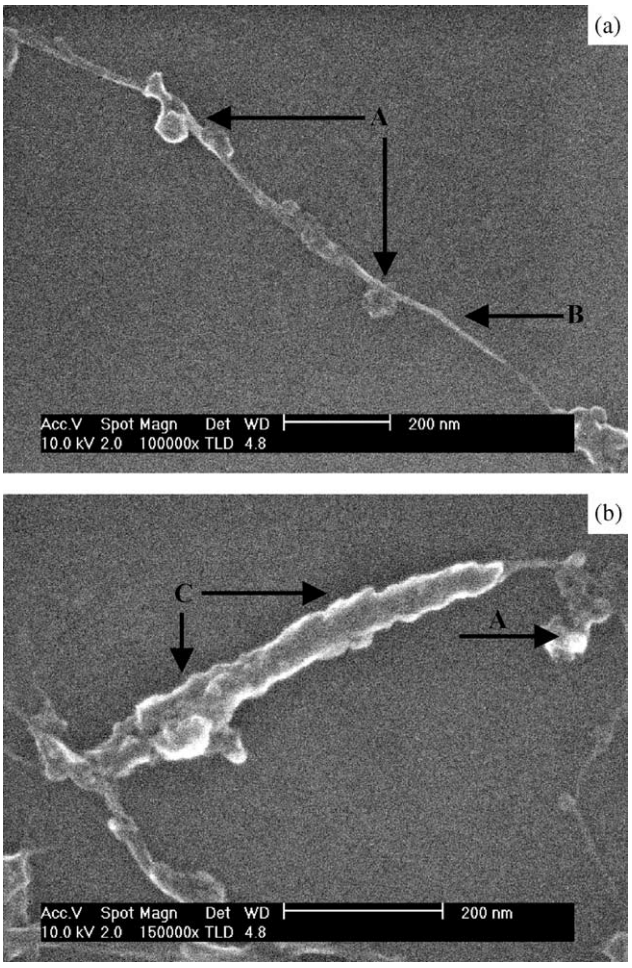

Fig. 5. SEM image of Py27D3. A, B, and C indicate the SWNT surfaces attached with dew-shaped polypyrrole particles, bare surfaces of SWNTs, and the surfaces covered with a polypyrrole thin film, respectively.

main chain of polypyrrole decomposes but SWNTs do not degrade until 800 °C in N_2 atmosphere. The polymer content in a sample is determined by using the residual weight difference between PPySWNTs and PPy. The actual content of PPy in the sample does not equal to the initial content of monomer but increases as the more monomer is added during polymerization. Polymer and nanotube contents are calculated from the residue at 800 °C and listed in Table 2.

The structure of PPySWNTs was determined by scanning electron microscopy (SEM). Fig. 5 shows SEM image of PPy27D3. There exist three different parts on the nanotube surfaces: (A) SWNT surfaces attached with spherical shape PPy of about 50 nm diameter, (B) bare surface of SWNT, and (C) the SWNT surfaces covered with thin film of PPy. A large proportion of polypyrrole attached on SWNT surfaces has the structure 'A'.

This could be explained by the following mechanism. Before polymerization, nanotube threads were dispersed by SDS and 1-pentanol in water. When pyrrole, DVB, and potassium persulfate (KPS) were added to the SWNTs-

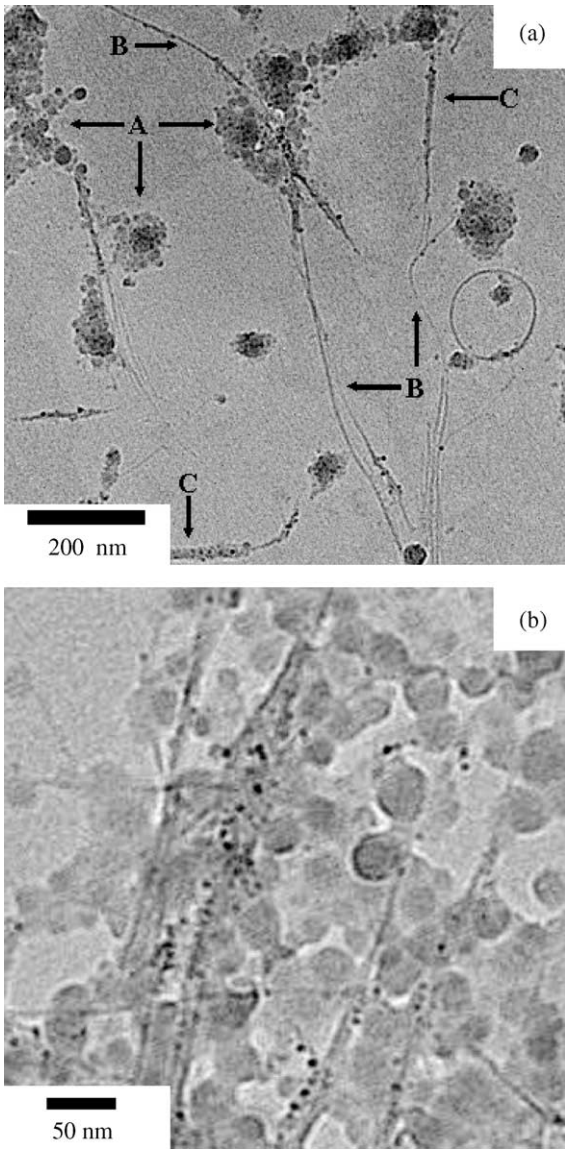

Fig. 6. (a) Low resolution and (b) high resolution TEM image of Py18D2.

surfactant dispersion, the ingredients diffused into two sites, (surfactant micelles and surfactant-stabilized nanotubes) due to their hydrophobic nature. Since the surfactant was added in large amount. There were surfactant micelles much larger in number than nanotubes and some surfactant micelles containing monomers were attached on nanotube surfaces forming dew shaped polypyrrole particles. Some of surfactant-stabilized nanotubes were covered with the thin film of polypyrrole. Some nanotube surfaces were not covered with polypyrrole.

Fig. 6 shows the structure of Py18D2. The sample for TEM analysis was prepared by depositing a Py18D2 on a carbon coated copper grid from the dispersion prepared by sonication for 5 h, blotting up by a filter paper to form a thin deposition and then evaporating the solvent slowly. We can also find the similar structure with SEM image in Fig. 5. The bare surface of SWNTs coexists with the covered SWNT

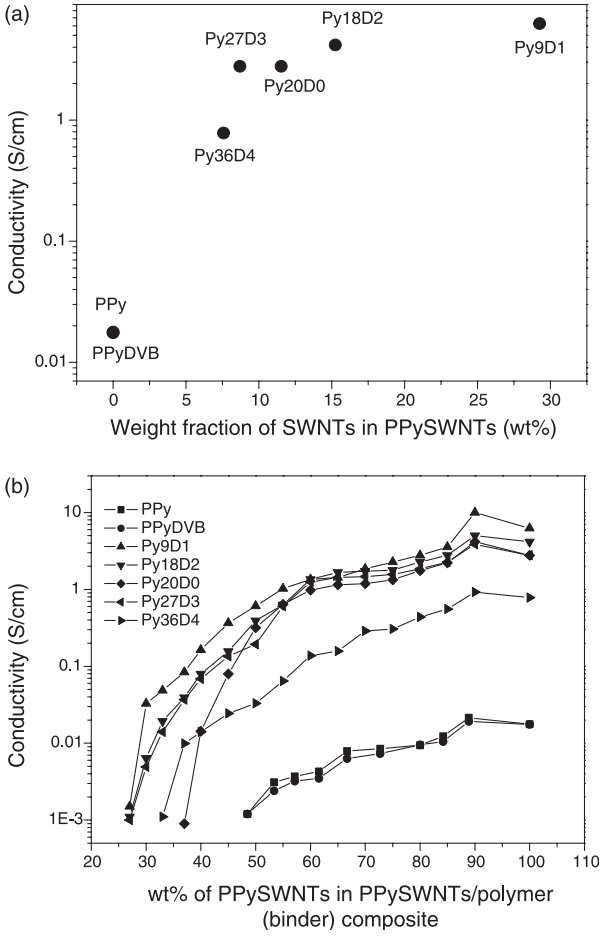

Fig. 7. Electrical conductivity of (a) PPySWNTs and (b) PPySWNTs/Kynar FLEX 2801 composites against the weight fraction of SWNTs.

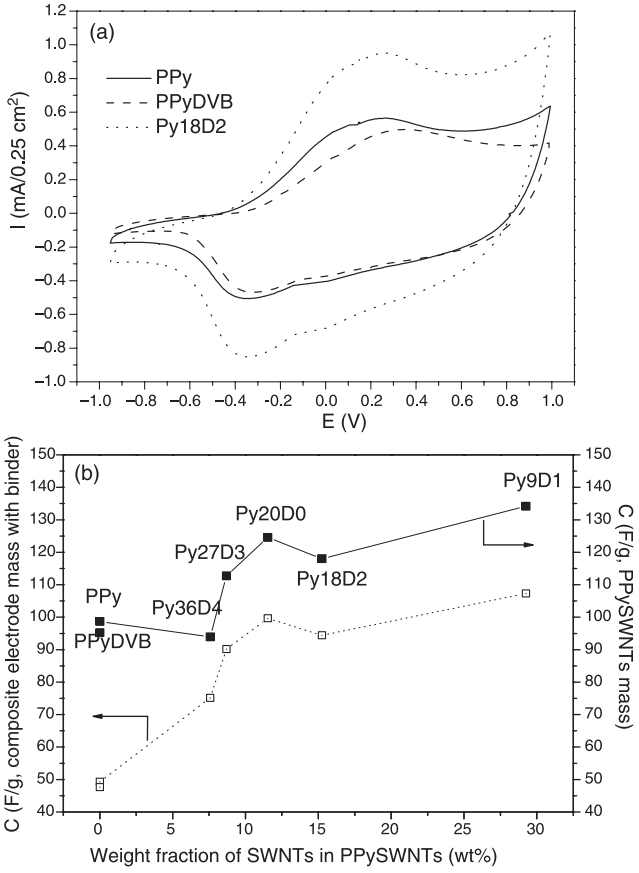

Fig. 8. (a) Cyclic voltammogram for PPy and PPyDVB electrode and (b) the specific capacitances of the PPySWNTs/Kynar FLEX 2801 composite electrode as a function of SWNTs loading fraction in PPySWNTs. Specific capacitance was calculated by dividing total electrode mass (left axis) and that per loading PPySWNTs weight (right axis) in (b).

surface by polypyrrole. Polypyrrole nanoparticles attached to the surface of SWNTs are shown in Fig. 6(b).

Fig. 7(a) shows the electrical conductivity for the PPy, PPyDVB, and PPySWNTs pellets made by pressing the powders. The PPy shows 0.0177 S/cm of electrical conductivity in Fig. 7(a). The weight fraction of SWNTs in each sample is listed on the Table 2. The conductivity increases sharply until the amount of SWNTs reaches 8.7 wt% in PPySWNTs. It seems that the percolation threshold of SWNTs is about 9 wt%. After the threshold, conductivity becomes higher as the weight fraction of SWNTs increases. When the weight fraction of SWNTs is 29.25 wt% (Py9D1), the conductivity is 6.25 S/cm. The composite of PPySWNTs and the binder, Kynar FLEX 2801, was made in the following way. The binder was added into PPySWNT powders. This mixture was dissolved in acetone and ground to prepare slurry. The slurry was cast on glass substrate and dried to make the composite film. Then it was baked to remove residual solvent at 60 °C for 4 h under vacuum. The electrical conductivity of each PPySWNTs/binder composite film was examined varying the weight fraction of binder in each composite. Fig. 7(b) shows the conductivity change due to the addition of binder in each sample. In our experiment, we could not examine the electric conductivity lower than 1×10^{-5} S/cm, because of the upper limit of resistance permitted by the equipment. So, almost all values start from 1×10^{-3} S/cm. The electrical conductivity of the composite containing Py36D4 and Py20D0, is reduced rapidly, when the amount of PPySWNTs becomes lower than 40 wt%. For the cases of other PPySWNTs, the percolation thresholds are about 30 wt%. The conductivity of the composite with PPyDVB shows similar or a little lower than that with PPy. The conductivity of each composite becomes higher as the amount of SWNTs in the composite increases. The 100 wt% PPySWNTs without binder shows little lower conductivity than the composite with 90 wt% of PPySWNTs, because of the sample preparation difference. The film was not formed when the weight fraction of PPySWNTs became 90%. So, the electrical conductivity was determined in pellet state.

Fig. 8(a) shows the cyclic voltammograms for the redox reaction of composite electrodes made from PPy, PPyDVB, and Py18D2 in 1 M $LiClO_4$ solution (EC:DMC = 1:1, by mole ratio). Carbon black (conducting material, super P black) was added with binder in the composite electrode to

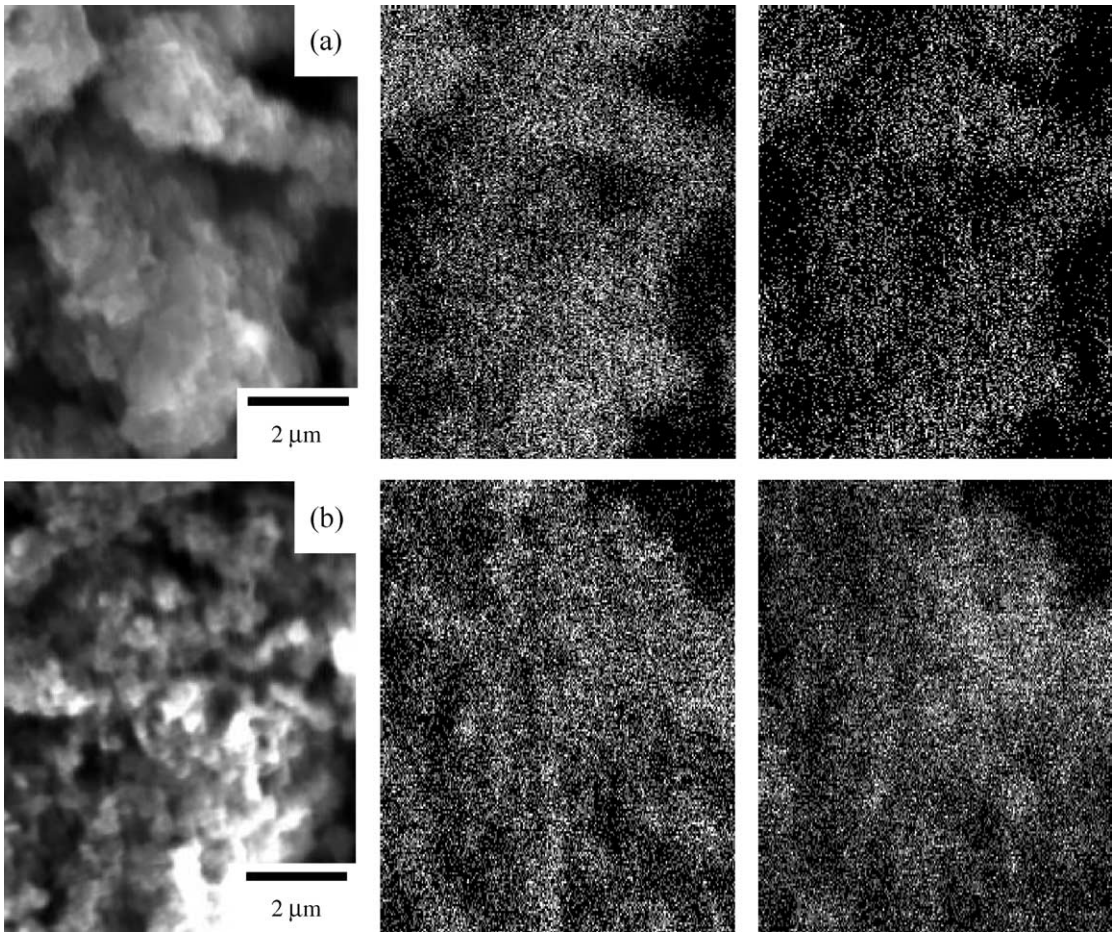

Fig. 9. SEM image (left picture) of the surface of composite electrode, and EDS pattern of the electrode surface taken by dot mapping method of fluorine (middle picture) and nitrogen (right picture), (a) for the electrode composed of PPy, binder, and active material (carbon black), and (b) for the electrode composed of Py9D1 and binder.

compensate the low electrical conductivity of PPy and PPyDVB. The weight ratio of composite electrode was 5:3:2 (PPy or PPyDVB:conducting material:binder). But, carbon black was not added in the PPySWNTs/binder composite electrode, because the electrical conductivity of PPySWNTs/binder composite was enough high to make an electrode. The weight ratio in composite electrode was 8:2 (PPySWNT:binder). The scan rate was 20 mV/s and the area of electrode was 0.25 cm^2. PPy shows the oxidation peak around ± 0.3 V. PPyDVB shows the peak shift toward positive voltage. The capacitance is calculated in the following equation.

$$C = \int \frac{i\Delta t}{\Delta V}$$

where C is the capacitance, i is current, V is voltage, and t is time [20].

Specific capacitance is plotted as a function of weight fraction of SWNTs in each PPySWNTs in Fig. 8(b). Fig. 8(b) shows the specific capacitance per total electrode mass on the left ordinate and that per PPySWNTs weight on the right ordinate. Two points at the 0 wt% of PPySWNTs represent the composite electrode composed of PPy and PPyDVB, respectively. The composite electrode with Py36D4 has low capacitance, because its electrical conductivity is low as shown in Fig. 7. PPy shows a little higher capacitance than PPyDVB. Therefore, Py20D0 has higher capacitance than other PPySWNTs except Py9D1. The specific capacitance becomes larger as the weight fraction of SWNTs in PPySWNTs increases. The specific capacitances of Py9D1 electrode per total electrode mass and per loading PPySWNTs weight are 108 and 134 F/g, respectively.

The electrode composed of PPy, PPyDVB and PPySWNTs was characterized by SEM and energy dispersive spectroscopy (EDS) pattern taken by dot mapping method to determine the surface morphology of the electrode and the dispersion of polypyrrole in the electrode. Fig. 9 shows an example of the electrode containing PPy and Py9D1. The weight fraction of polypyrrole molecule in each electrode was 50 wt% for PPy and 56.6 wt% for Py9D1. Three images in Fig. 9 represent surface morphology, dispersion states of fluorine (F), and nitrogen (N) atoms in the composite electrodes of

PPy, and Py9D1. The binder used here, Kynar FLEX 2801, has fluorine atom in the molecule. So, the adapted images of fluorine and nitrogen atoms illustrate the distributions of the binder molecule and PPy, respectively. The electrode composed of Py9D1 exhibit more porous structure on the surface and more polypyrrole molecule on the surface of the electrode than the electrode composed of PPy, as shown in SEM pictures. This could be explained that SWNTs played a role as a template for the dispersion of polypyrrole on the surface of the electrode.

4. Conclusion

In summary, the SWNTs covered with polypyrrole nanoparticles were obtained via in situ miniemulsion polymerization of pyrrole monomer. Electrical conductivity of PPySWNTs was higher than pristine polypyrrole. The PPySWNT/Kynar 2801 composite electrode showed higher electric conductivity than polypyrrole/Kynar2801 composite. PPySWNTs showed electrochemical redox behavior without adding carbon black. PPySWNTs/binder composite electrode had larger specific capacitance as the weight fraction of SWNTs increased. It showed higher specific capacitance than polypyrrole/binder/carbon black because it had more porous structure and bare nanotube surfaces.

Acknowledgements

Authors would like to express their sincere thanks to KOSEF (Korea Science and Engineering Foundation), to CAFPoly (Center for Advanced Functional Polymers), and to the BK 21 program for their financial support. And Dr Kim Sun Ha at the KBSI (Daegu) is thanked for taking the solid state 400 MHz NMR data.

References

[1] Iijima S, Ichihashi T. Nature 1993;363:603–5.
[2] Dresselhaus MS, Dresselhaus G, Eklund PC. Science of fullerenes and carbon nanotubes. San Diego, CA, USA: Academmic Press; 1996.
[3] Wong EW, Sheehan PE, Lieber CM. Science 1997;277:1971–5.
[4] Ebbesen TW. Carbon nanotubes. Boca Raton: CRC Press; 1997.
[5] Ajayan PM. Chem Rev 1999;99:1787–99.
[6] Rao CNR, Satishkumar BC, Govindaraj A, Nath M. Chem Phys Chem 2001;2:78–105.
[7] Baughman RH, Zakhidov AA, de Heer WA. Science 2002;297: 787–92.
[8] Dai HJ. Acc Chem Res 2002;35:1035–44.
[9] Tasis D, Tagmatarchis N, Georgakilas V, Prato M. Chem Eur J 2003; 9:4001–8.
[10] Hirsch A. Angew Chem Int Ed 2002;41:1853–9.
[11] Ham HT, Koo CM, Kim SO, Choi YS, Chung IJ. Macromol Res 2004; 12:384–90.
[12] Xia HS, Wang Q, Qiu GH. Chem Mater 2003;15:3879–86.
[13] Liu ZM, Dai XH, Xu J, Han BX, Zhang JL, Wang Y, et al. Carbon 2004;42:458–60.
[14] Stra A, Stoddart JF, Steuerman D, Dichl M, Boukai A, Wong EW, et al. Angew Chem Int Ed 2001;40:1721–5.
[15] Hashmi SA, Latham RJ, Linford RG, Schlindwein WS. Polym Int 1998;47:28–33.
[16] Mastragostino M, Arbizzani C, Soavi F. J Power Sources 2001;97/98: 812–5.
[17] Arbizzani C, Mastragostino M, Meneghello L. Electrochim Acta 1996;41:21–6.
[18] Gofer Y, Sarker H, Killian JG, Poehler TO, Searson PC. Appl Phys Lett 1997;71:1582–4.
[19] Ryu KS, Kim KM, Park NG, Park YJ, Chang SH. J Power Sources 2002;103:305–9.
[20] Park JH, Park OO. J Power Sources 2002;111:185–90.
[21] Niu C, Sichel EK, Hoch R, Moy D, Tennent H. Appl Phys Lett 1997; 70:1480–2.
[22] An KH, Kim WS, Park YS, Moon JM, Bae DJ, Lim SC, et al. Adv Funct Mater 2001;11:387–92.
[23] Frackowiak E, Metenier K, Bertagna V, Beguin F. Appl Phys Lett 2000;77:2421–3.
[24] Jurewicz K, Delpeux S, Bertagna V, Beguin F, Frackowiak E. Chem Phys Lett 2001;347:36–40.
[25] Hughes M, Shaffer MSP, Renouf AC, Singh C, Chen GZ, Fray DJ, et al. Adv Mater 2002;14:382–5.
[26] Park JH, Ko JM, Park OO. J Electrochem Soc 2003;150:A864–A7.
[27] Callegari A, Cosnier S, Marcaccio M, Paolucci D, Paolucci F, Georgakilas V, et al. J Mater Chem 2004;14:807–10.
[28] Piirma I. Emulsion polymerization. New York: Academic Press; 1976.
[29] Atik SS, Thomas JK. J Am Chem Soc 1981;103:4279.
[30] Landfester K. Macromol Rapid Commun 2001;22:896–936.
[31] Asua JM. Prog Polym Sci 2002;27:1283–346.
[32] Gangopadhyay R, De A. Chem Mater 2000;12:608–22.
[33] Jang J, Lee K. Chem Commun 2002;10:1098–9.
[34] Rinzler AG, Liu J, Dai H, Nikolaev P, Huffman CB, Rodriguez-Macias FJ, et al. Appl Phys A: Mater Sci Proc 1998;67:29–37.
[35] Joseph R, Ford WT, Zhang S, Tsyurupa MP, Pastukhov AV, Davankov VA. J Polym Sci Part A: Polym Chem 1997;35:695–701.
[36] Forsyth M, Truong VT, Smith ME. Polymer 1994;35:1593–601.